# Properties of the ground $^3F_2$ state and the excited $^3P_0$ state of atomic thorium in cold collisions with $^3$He

Yat Shan Au,[1,3] Colin B. Connolly,[1,3] Wolfgang Ketterle,[2,3] and John M. Doyle[1,3]
[1]*Department of Physics, Harvard University, Cambridge, Massachusetts 02138, USA*
[2]*Department of Physics, Massachusetts Institute of Technology, Cambridge, Massachusetts 02139, USA*
[3]*Harvard-MIT Center for Ultracold Atoms, Cambridge, Massachusetts 02138, USA*
(Received 20 March 2014; published 3 September 2014)

Inelastic cross sections for collisions between thorium (Th) and helium ($^3$He) are measured. For Th[$^3F_2$]–$^3$He, we determine the ratio of momentum transfer to Zeeman relaxation cross sections to be $\gamma \sim 500$ at 800 mK. For Th[$^3P_0$]–$^3$He, we find no quenching of this metastable state during $10^6$ collisions. We measure the radiative lifetime of Th[$^3P_0$] to be $\tau > 130$ ms. The observed stability of Th[$^3P_0$] opens up the possibility of trapping this metastable species.

DOI: 10.1103/PhysRevA.90.032702 PACS number(s): 34.50.Cx, 37.10.De, 32.60.+i

## I. INTRODUCTION

The widening variety of atoms used in ultracold physics research provides new opportunities in research areas as diverse as clocks, searches for physics beyond the standard model, and quantum simulation. The use of rare earth atoms has enabled the realization of novel dipolar interactions [1,2] and the development of new schemes for encoding quantum information [3]. Alkaline earth atoms are competitive contestants to be the next-generation metrological standards [4] and provide new collisional physics particular to highly stable metastable states [5,6]. As a platform for understanding these new cold atomic systems, atom-helium (He) collisions often provide useful links between theory and experiments, due to the relatively simple electronic structure and low polarizability of He. The study of atom collisions with He has led to a better understanding of electrostatic anisotropy [5–7], spin-orbit coupling [8,9], and shielding by outer $s$ electrons [10,11] in cold collisions.

Electrostatic anisotropy plays a crucial role in collisions of non-$S$-state atoms. During a collision, anisotropic interactions can effectively couple different projections within an orbital angular momentum $l_m$ manifold and, hence, change the orientation of the magnetic moment (Zeeman relaxation). The ratio $\gamma$ between the momentum transfer and the Zeeman relaxation cross sections is a useful quantity characterizing such collisions. Considering benchmark examples of $\gamma$ in collisions with He, for the oxygen atom [$^3P_2$], $\gamma \sim 7$ [12], compared to the $S$-state potassium atom, for which $\gamma > 10^8$ [13]. For some atoms, like the rare earths, the presence of outer $s$ electrons in non-$S$-state atoms can suppress ("shield") electrostatic anisotropy, resulting in $\gamma > 10^4$ [14,15].

In this paper, we use atomic thorium (Th) to study the effects of possible shielding in the actinides, the first study of its kind. In doing so, we extend previous studies of electrostatic anisotropy suppression in transition metals [14] and in lanthanides [15], thus providing quantitative comparison of the degree of outer $s$-electron shielding between $3d4s$ (e.g., Ti), $4f6s$ (e.g., Tm), and $6d7s$ (e.g., Th) systems.

In addition to our study of anisotropy in the ground state, we also measure the collisional properties of Th in its first excited $^3P_0$ state. Recently, there has been interest in understanding $^1S_0$-$^3P_0$ collisions [16–18]. In our experiment, transitions between fine-structure multiplets are not energetically allowed. This permits direct study of metastable electronic quenching. We find that this metastable state of Th has a very long lifetime, apparently not strongly affected by relativistic perturbations in this heavy complex atom.

## II. EXPERIMENTAL SETUP

The core approach for all of our work is the creation of cold, dilute gases of Th in the presence of cold $^3$He gas, the collisional partner species. We prepare cold samples of atomic Th ($>10^{11}$) using buffer-gas cooling [19]. Our setup consists of a copper cell at 800 mK, cooled by a dilution refrigerator via a flexible heat link [20]. A pair of superconducting Helmholtz coils can create a uniform magnetic field over the cell region for Zeeman relaxation measurements. (No magnetic field is applied for the excited $^3P_0$-state experiments.)

Atomic Th is introduced into the buffer gas via laser ablation of a solid Th metal target. Thorium atoms thermalize to the cell temperature via collisions with $^3$He before diffusing to the cell wall, where they stick. We directly measure the atoms' temperature by fitting optical absorption spectra of the $6d^27s^2$ ($^3F_2$) $\rightarrow$ $6d^27s7p$ ($^3G_3$) transition at 372 nm to a Voigt profile. We make measurements at times later than the diffusive decay time constant, at which point the single-exponential decay profile of the Th ($^3F_2$) optical density indicates that all but the lowest diffusion mode can be ignored [19]. In this case, the diffusion time constant $\tau_d$ in a cylindrical cell of radius $r$ and length $L$ is given by

$$\tau_d = \frac{32}{3\pi}\frac{n_b\sigma_d}{\bar{v}}\left(\frac{j_{01}^2}{r^2}+\frac{\pi^2}{L^2}\right)^{-1}, \quad (1)$$

where $n_b$ is the buffer-gas density, $\sigma_d$ is the thermally averaged momentum-transfer cross section, $j_{01} \approx 2.4$ is the first 0 of the Bessel function $J_0$, and $\bar{v}$ is the mean Th-$^3$He center of mass speed [21].

## III. MEASURING ZEEMAN RELAXATION

To measure Zeeman relaxation, we apply a uniform magnetic field of up to 2 T to spectroscopically resolve the Zeeman sublevels ($m_J$ states) of the Th ground $^3F_2$ state, which we probe using the 372-nm transition. We drive the system

 

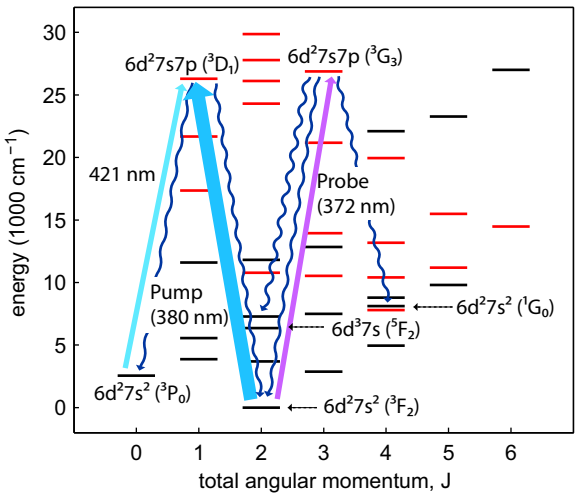


FIG. 1. (Color online) Energy levels of thorium up to 30 000 cm$^{-1}$ [22]. The black (red) line indicates the even-parity (odd-parity) state. In the Zeeman relaxation measurement, the ground $^3F_2$ state is pumped by the $6d^27s^2\ (^3F_2) \rightarrow 6d^27s7p\ (^3D_1)$ transition at 380 nm and probed by the $6d^27s^2\ (^3F_2) \rightarrow 6d^27s7p\ (^3G_3)$ transition at 372 nm. In the excited $^3P_0$ measurements, the $^3P_0$ state is populated by optical pumping via $6d^27s7p\ (^3D_1)$ and is probed using the $6d^27s^2\ (^3P_0) \rightarrow 6d^27s7p\ (^3D_1)$ transition at 421 nm.

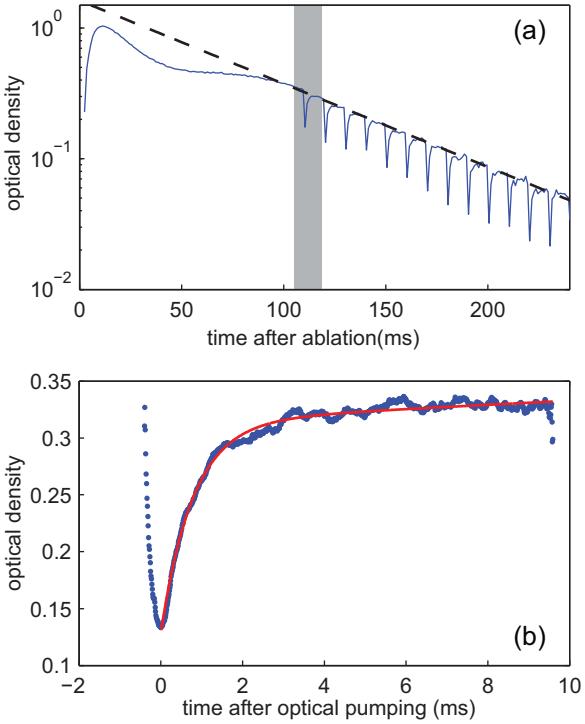


FIG. 2. (Color online) (a) The optical density (OD) of atomic thorium during a Zeeman relaxation measurement. Measurements were performed starting 100 ms after ablation, when both diffusion modes and temperature stabilized, as verified by the simple exponential decay of the atomic OD (dashed line). (b) Data corresponding to the shaded area in (a) after subtraction of the diffusive baseline, showing the depletion of the OD by optical pumping and recovery of the OD via inelastic collisions. Multiple measurements were made with separate optical pumping pulses before the atoms diffused to the cell wall.

away from thermal equilibrium and then monitor the repopulation from other Zeeman sublevels via inelastic collisions. Specifically, we deplete a high-field-seeking (HFS) $m_J > 0$ state via an optical pumping pulse using the $6d^27s^2\ (^3F_2) \rightarrow 6d^27s7p\ (^3D_1)$ transition at 380 nm, as shown in Fig. 1.

The Zeeman shift of an atomic transition can be calculated from the Landé $g$ factors, $g_J$, of the terms of the lower and the upper state,

$$g_J \approx \frac{3}{2} + \frac{S(S+1) - L(L+1)}{2J(J+1)}, \tag{2}$$

if both orbital and spin angular momentum quantum numbers $L$ and $S$ are good quantum numbers for the states. The literature value for Th ($^3F_2$) is $g_J = 0.736$ [23], compared to the $g_J = 2/3$ predicted by Eq. (2). The discrepancy is not unexpected for heavy atoms, and it suggests a significant relativistic perturbation to the atomic states, which can affect the cold collisional properties [8]. From our spectroscopic measurements, we infer $g$ factors for the excited $^3D_1$ and $^3G_3$ states (Table I), which have not been previously reported.

The method used here for measuring the cross-section ratio $\gamma$, i.e., observing the recovery of HFS states, is different from that used in [20], which relies on monitoring the decay of a low-field-seeking state populated during the initial laser ablation. In the latter case, measurements made soon after ablation are complicated by high-order diffusion modes and thermal effects from the laser ablation, limiting the sensitivity of that method to $\gamma \gtrsim 1000$ [24].

In this work, the use of optical pumping to drive the system out of equilibrium allows us to perform the measurements after the decay of high-order diffusion modes and the establishment of thermal stabilization, while preserving the sensitivity to short time scales. We verify that the necessary experimental conditions are met by observation of the simple exponential decay of the atomic optical density during the measurements. This method thus enables a measurement of $\gamma$ to values as low as $\approx$1. Additionally, optical pumping allows a higher data rate by enabling repetition of relaxation measurements within the atoms' diffusive lifetime (see Fig. 2) and provides a way to check for possible effects of the ablation pulse on the measurement [9,10].

The observed time constant $\tau_Z$ for repopulation of the HFS state via inelastic collisions is given by [25]

$$\tau_Z = \frac{32}{3\pi}\frac{\gamma}{\bar{v}^2\tau_d}\left(\frac{j_{01}^2}{r^2} + \frac{\pi^2}{L^2}\right)^{-1}. \tag{3}$$

TABLE I. Measured $g$ factors. We deduce that $g$ factors of the excited states are from the observed Zeeman shifts. Frequency shifts were measured using a wave meter. The uncertainty in $g_J$ is dominated by the current-to-field calibration of the magnetic field coils.

| Level (cm$^{-1}$) | Term | $g_J$ [Eq. (2)] | $g_J$ (observed) |
|---|---|---|---|
| 0 | $^3F_2$ | 0.667 | 0.736 [23] |
| 26 287.049 | $^3D_1$ | 0.5 | $0.90 \pm 0.05$ (this work) |
| 26 878.162 | $^3G_3$ | 0.75 | $1.10 \pm 0.05$ (this work) |

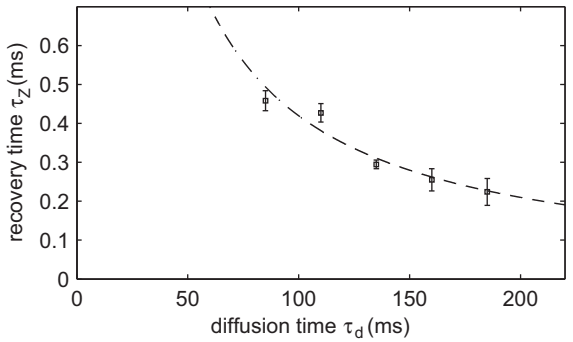


FIG. 3. Zeeman relaxation measurement. Fitted repopulation time $\tau_Z$ of the most high-field-seeking state ($m_J = J$) of Th at different $^3$He densities ($\tau_d \propto n_{\mathrm{He}}$) and 0.5 T. Error bars are statistical uncertainties. The ratio $\gamma$ of the momentum transfer to Zeeman relaxation cross sections is obtained by fitting to Eq. (3).

We determine $\gamma$ by fitting our measurements of $\tau_Z$ and $\tau_d$ to Eq. 3, which shows good agreement with the data (Fig. 3).

At finite temperature, an inelastic collision can sometimes have sufficient energy to promote a Th atom from the stretched HFS state to higher sublevels, slowing the relaxation to equilibrium and resulting in an overestimation of $\gamma$. We simulated this process in our system using the model developed in [20]. In Fig. 4, the upper limit of the error bars is statistical uncertainty, while the lower limit represents uncertainty due to such thermal excitations.

We also repeat the Zeeman relaxation measurement on the ground-state sublevel with $m_J = J - 1$ at 0.5 T and find $\gamma$ to be statistically equivalent to that of the most HFS state ($m_J = J$). We could not make this comparison at higher magnetic fields due to the insufficient thermal population of the $m_J = J - 1$ state.

A source of possible measurement error is the filling of the HFS state from long-lived states (e.g., $^5F_2$; see Fig. 1) populated during optical pumping via nonzero branching from the excited $^3D_1$ state. The state lifetimes and transition strengths are not sufficiently known to quantify the populations of other excited states or the rate of decay into the ground state. However, the populations in such states due to optical pumping will depend sensitively on both the power and the duration of the pump and probe lasers. We change these parameters by a factor of 2 and obtain statistically equivalent values of $\gamma$. Therefore, we conclude that decay from other states does not significantly affect our measurement.

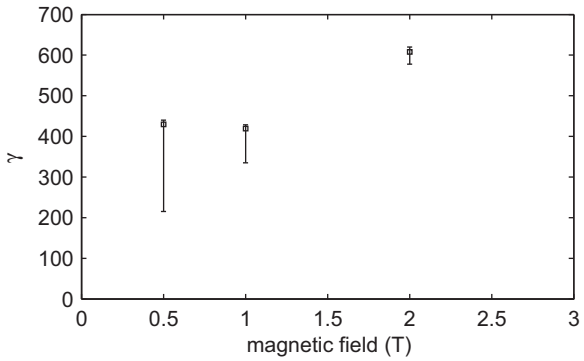


FIG. 4. Momentum transfer to the Zeeman relaxation collision ratio $\gamma$ for the Th ($^3F_2$) ground state, measured at 800 mK.

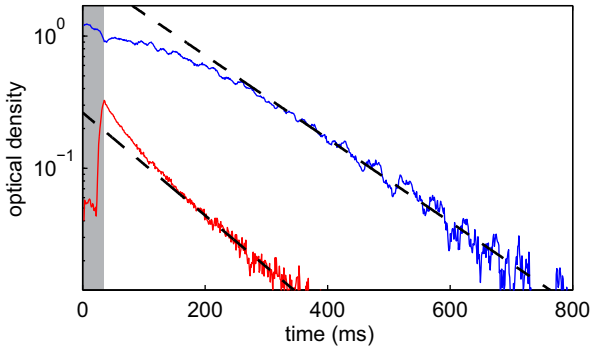


FIG. 5. (Color online) The optical density (OD) of atomic thorium during the excited $^3P_0$-state measurement. Blue (red) shows the OD of the $^3F_2$ ($^3P_0$) state. Optical pumping is applied in the first 20 ms [shaded (gray) area] to transfer the population from the ground $^3F_2$ state to the excited $^3P_0$ state. Dashed lines are single-exponential fits to the lowest diffusion mode at late times. Diffusive fits start at 310 and 180 ms for the $^3P_0$ and the $^3F_2$ state, respectively.

## IV. EXCITED $^3P_0$ STATE

We also apply the optical pump and probe technique to study collisions in the metastable first excited $^3P_0$ state of Th. The state is probed using the $6d^27s^2$ ($^3P_0$) $\rightarrow$ $6d^27s7p$ ($^3D_1$) transition at 421 nm. When the cold Th gas is produced via laser ablation, a small fraction occupies the $^3P_0$ state. We increase the $^3P_0$ state population by an order of magnitude using optical pumping via $6d^27s7p$ ($^3D_1$) (see Figs. 1 and 5). We measure the subsequent decay time of the $^3P_0$ state at various buffer-gas densities to search for collisional quenching of the excited state. The results are shown in Fig. 6. The excited $^3P_0$-state lifetime $\tau_P$ shows a linear dependence on the ground-state ($^3F_2$) diffusion time $\tau_F$, which is proportional to the buffer-gas density.

We check for refilling of the $^3P_0$ state from upper reservoir states. We probe the $^3P_0$ state with sufficient laser power so that $\tau_P$ is determined by optical pumping instead of diffusion or radiative decay. We shutter the probe beam for 100 ms before probing the state again. We do not observe a recovery of the

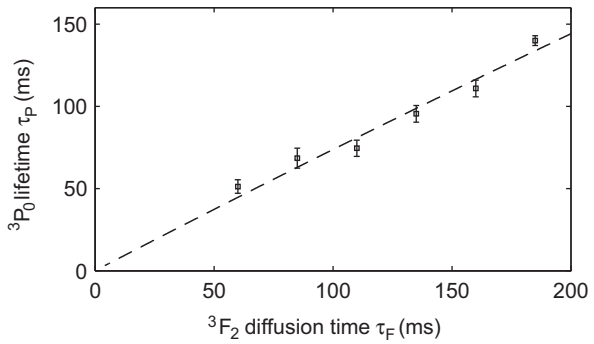


FIG. 6. Linear dependence of the excited $^3P_0$-state lifetime, $\tau_P$.

$^3P_0$ population, and thus we conclude that the contribution to $\tau_P$ by refilling from a reservoir is insignificant.

Collisional quenching would cause a negative slope of $\tau_P$ vs $\tau_F$. Radiative decay would limit $\tau_P$ to a finite value. Neither effect appears in our data, which display a positive linear dependence of $\tau_p$ on $\tau_F$. Therefore, we conclude that no electronic quenching collisions were observed. Using the highest buffer-gas density data point, we bound the value of $\gamma > 10^6$ and the radiative lifetime of the state $\tau_R > 130$ ms.

## V. CONCLUSION

We measure the ratio $\gamma$, the momentum transfer to Zeeman relaxation cross sections, of Th [$^3F_2$] in collisions with He. We find that $\gamma \approx 500$, which is well above that of open-shell oxygen [12] but below that of submerged-shell lanthanides [15]. This value of $\gamma$ is too small for direct buffer-gas loading into a magnetic trap [26], but it is sufficient for indirect loading from a buffer-gas beam [27]. This would allow for the study of trapped, cold atomic Th, perhaps opening up the actinides to cold-atom physics studies and precision measurements.

We also study metastable Th in the first excited $^3P_0$ state, setting a lower bound of $\gamma > 10^6$ for electronic quenching in collisions with He of the first excited $^3P_0$ state. Our result is similar to previous studies of $^1S_0$-$^3P_0$ collisions among the alkaline earths [16–18]. This very low quenching cross section allows for the determination of a long radiative lifetime for Th ($^3P_0$), $\tau > 130$ ms. This invites the possibility of studying ultracold metastable Th in an optical lattice, as was done with the lanthanide Yb [7].

## ACKNOWLEDGMENTS

We acknowledge Timur Tscherbul for helpful theoretical input and Elizabeth Petrik for assistance in target preparation. This work was supported by the NSF through the Harvard-MIT Center for Ultracold Atoms.

[1] M. Lu, N. Q. Burdick, and B. L. Lev, Phys. Rev. Lett. **108**, 215301 (2012).
[2] K. Aikawa, A. Frisch, M. Mark, S. Baier, A. Rietzler, R. Grimm, and F. Ferlaino, Phys. Rev. Lett. **108**, 210401 (2012).
[3] M. Saffman and K. Molmer, Phys. Rev. A **78**, 012336 (2008).
[4] A. D. Ludlow, T. Zelevinsky, G. K. Campbell, S. Blatt, M. M. Boyd, M. H. G. de Miranda, M. J. Martin, J. W. Thomsen, S. M. Foreman, J. Ye *et al.*, Science **319**, 1805 (2008).
[5] D. Hansen and A. Hemmerich, Phys. Rev. Lett. **96**, 073003 (2006).
[6] V. Kokoouline, R. Santra, and C. H. Greene, Phys. Rev. Lett. **90**, 253201 (2003).
[7] A. Yamaguchi, S. Uetake, D. Hashimoto, J. M. Doyle, and Y. Takahashi, Phys. Rev. Lett. **101**, 233002 (2008).
[8] S. E. Maxwell, M. T. Hummon, Y. Wang, A. A. Buchachenko, R. V. Krems, and J. M. Doyle, Phys. Rev. A **78**, 042706 (2008).
[9] C. B. Connolly, Y. S. Au, E. Chae, T. V. Tscherbul, A. A. Buchachenko, H.-I. Lu, W. Ketterle, and J. M. Doyle, Phys. Rev. Lett. **110**, 173202 (2013).
[10] M.-J. Lu, V. Singh, and J. D. Weinstein, Phys. Rev. A **79**, 050702(R) (2009).
[11] C. B. Connolly, Y. S. Au, S. C. Doret, W. Ketterle, and J. M. Doyle, Phys. Rev. A **81**, 010702 (2010).
[12] R. V. Krems and A. Dalgarno, Phys. Rev. A **68**, 013406 (2003).
[13] T. V. Tscherbul, P. Zhang, H. R. Sadeghpour, A. Dalgarno, N. Brahms, Y. S. Au, and J. M. Doyle, Phys. Rev. A **78**, 060703(R) (2008).
[14] C. I. Hancox, S. C. Doret, M. T. Hummon, L. Luo, and J. M. Doyle, Nature **431**, 281 (2004).
[15] C. I. Hancox, S. C. Doret, M. T. Hummon, R. V. Krems, and J. M. Doyle, Phys. Rev. Lett. **94**, 013201 (2005).
[16] C. Lisdat, J. S. R. V. Winfred, T. Middelmann, F. Riehle, and U. Sterr, Phys. Rev. Lett. **103**, 090801 (2009).
[17] M. Bishof, M. J. Martin, M. D. Swallows, C. Benko, Y. Lin, G. Quemener, A. M. Rey, and J. Ye, Phys. Rev. A **84**, 052716 (2011).
[18] S. Uetake, R. Murakami, J. M. Doyle, and Y. Takahashi, Phys. Rev. A **86**, 032712 (2012).
[19] R. deCarvalho, J. M. Doyle, B. Friedrich, T. Guillet, J. Kim, D. Patterson, and J. D. Weinstein, Eur. Phys. J. D **7**, 289 (1999).
[20] C. Johnson, B. Newman, N. Brahms, J. M. Doyle, D. Kleppner, and T. J. Greytak, Phys. Rev. A **81**, 062706 (2010).
[21] J. Hasted, *Physics of Atomic Collisions* (Butterworth & Co Publishers Ltd, Washington, DC, 1972).
[22] C. Corliss and W. Bozman, *NBS Monograph 53* (U.S. Department of Commerce, Washington, DC, 1962).
[23] J. J. Katz and G. T. Seaborg, *The Chemistry of the Actinide Elements* (John Wiley and Sons, Inc., New York, 1957).
[24] C. B. Connolly, Ph.D. thesis, Harvard University, 2012.
[25] C. B. Connolly, Y. S. Au, E. Chae, T. V. Tscherbul, A. A. Buchachenko, W. Ketterle, and J. M. Doyle, Phys. Rev. A **88**, 012707 (2013).
[26] R. de Carvalho and J. Doyle, Phys. Rev. A **70**, 053409 (2004).
[27] H.-I. Lu, J. Rasmussen, M. J. Wright, D. Patterson, and J. M. Doyle, Phys. Chem. Chem. Phys. **13**, 18986 (2011).